## COORDINATION COMPOUNDS

# Volatile β-diketonate complexes of Rb-Co: effect of incorporation a neutral ligand 18-crown-6 ether

**D. V. Kochelakov[a, *], P. S. Stabnikov[a], E. S. Vikulova[a]**

[a]*Nikolaev Institute of Inorganic Chemistry, Siberian Branch of Russian Academy of Sciences, Novosibirsk, 630090 Russia*

**e-mail: pi-3@outlook.com*

Received August 05, 2024

Revised October 01, 2024

Accepted October 09, 2024

Heterometallic β-diketonate complexes $M^I[M(L)_n]$ containing alkali metal cations $M^I$ are of great interest from the point of view of their use in the preparation of halide perovskites. However, such compounds are poorly studied for $M^I$ = Rb and there is no information on their crystal structure. In this work, two types of such complexes are presented: $Rb[Co(hfac)_3]$ **1** and novel $[Rb(18C6)][Co(hfac)_3]$ **2** (hfac = $CF_3COCHCOCF_3^-$, hexafluoroacetylacetonate ion, 18C6 = 18-crown-6 ester). The compounds were characterized by elemental analysis, IR spectroscopy, single-crystal and powder XRD, and TGA. Both complexes have a chain polymeric structure, whereas the inclusion of the neutral 18C6-ligand effectively reduces the number of contacts between the cation and the complex anion $[Co(hfac)_3]^-$. Both heterometallic complexes are more thermally stable than Rb(hfac), with **1** partially transitioning into the gas phase at atmospheric pressure.

*Keywords:* heterometallic complexes, rubidium, cobalt, hexafluoroacetylacetonate, X-ray diffraction analysis, thermal properties, fluoroperovskites

**DOI:** 10.31857/S0044457X250107e2

## INTRODUCTION

Recently, fluoroperovskites of the type $M^IM^{II}F_3$ ($M^I$ – alkali metal cation) have attracted increasing attention due to their unique properties. For example, they are promising as components of solar cells [1, 2], light-emitting devices [3, 4], and photocatalytic systems [5, 6]. Interest in them is associated with the increased stability of inorganic perovskites to moisture compared to analogues that include

organic cations [7]. By varying the metals $M^{I}$ and $M^{II}$, compounds with diverse properties can be obtained [8]. The most widely studied are Rb-containing perovskites, among which, according to calculations, interesting magnetic and electronic properties for application in spintronics are expected for $RbCoF_3$ [9–11]. With a band gap of 4.10–4.60 eV, relatively high values of magnetic moment $\mu = 3.0$ A $m^2$ are predicted for it [8]. It should be noted that experimental data confirm the presence of antiferromagnetic properties [12, 13], found in theoretical works.

Similar compounds are usually obtained by melting halides at high temperatures (>800°C) or by solution microwave synthesis in expensive equipment (mainly due to the corrosive nature of fluorides) [14]. To mitigate synthesis conditions, it is necessary to transition to organometallic precursors. Using the example of bimetallic trifluoroacetates [15, 16], it has been shown that alkali metal fluoroperovskites can be obtained above ~250 °C by both solid-state and solution methods. Chemical vapor deposition ($M^{I}M^{II}F_3$ systems, allowing for high uniformity of coatings on objects with complex geometry [17]. For MOCVD application, the heterometallic precursor must possess volatility and thermal stability. In particular, the fluorinated **MOCVD** ) is also promising for obtaining M β -diketonate $K[Mn(hfac)_3]$ (hfac – 1,1,1,5,5,5-hexafluoropentanedionate-2,4) was successfully used to obtain $KMnF_3$ films on an MgO substrate [17]. However, similar compounds for Rb and Cs have not been sufficiently studied, and examples of vapor deposition of Co-containing fluoroperovskites are absent.

It should be noted that complexes $M^{I}[Co(hfac)_3]$, where $M^{I}$= K, Rb, Cs, were obtained in the 1970s by the scientific group of M.Z. Gurevich and Prof. B.D. Stepin [18, 19], and their thermal properties were investigated by various methods. However, data on the study of synthesis products for $M^{I}$= K, Rb are not presented, and the values of saturated vapor pressure appear to be overestimated, probably due to the method used, as the isoteniscopic method allows contact of complex vapors

with mercury in the manometer [20]. Later [21], it was established that the $K[Co(hfac)_3]$ complex has a chain polymer structure.

To reduce the number of interactions within the chains, which could contribute to increasing the volatility of such complexes, in 2018 it was proposed to use an additional neutral polydentate ligand [22], in particular, it was shown that $[Na(tetraglyme)][M^{III}(hfac)_4]$ (tetraglyme - 2,5,8,11,14-pentaoxapentadecane, $M^{III}$ = Y, Gd) is an effective MOCVD precursor for obtaining the corresponding $NaM^{III}F_4$ films [22]. However, the number of donor atoms in tetraglyme may not be sufficient to saturate the coordination sphere of a cation with a larger ionic radius. In addition, the steric lability of glymes leads to the coordination of neighboring cations, strengthening the chain structures, as demonstrated by the example of $K^+$ [23]. In this regard, for the synthesis of heterometallic complexes with a reduced number of interactions between the cation $M^I$ = $K^+$, $Rb^+$, $Cs^+$ we propose to use sterically rigid molecules with a large number of donor atoms, in particular crown ethers. Previously, heterometallic β -diketonates with 18-crown-6 ether were not known.

This paper presents the first comparison of the structure and thermal properties of heterometallic complexes of both types: $Rb[Co(hfac)_3]$ and the new $[Rb(18C6)][Co(hfac)_3]$ (18C6 - 18-crown-6 ether).

## EXPERIMENTAL PART

**Materials and methods.** The reagents used were $Rb_2CO_3$ (≥0.99), $Co(NO_3)_2 \cdot 6H_2O$ (≥0.99), 18C6 (≥0.99), and H(hfac) (≥0.99); diethyl ether (purity ≥0.98) and dichloromethane (≥0.99) were used as solvents. The synthesis and purification of the initial complexes $[Co(H_2O)_2(hfac)_2]$ and Rb(hfac) were carried out according to the methods [24, 25]. IR absorption spectra (400–4000 $cm^{-1}$) of the synthesis products in the form of KBr tablets or suspensions in fluorinated oil were recorded on a Scimitar FTS 2000 spectrometer. Band assignments were made by comparison with

literature data [25, 26]. Elemental analysis of the samples was carried out at the Chemical Research Center for Collective Use of the SB RAS (Novosibirsk, NIOCH SB RAS). Standard errors in determining the content of C, H, and F do not exceed 0.5 wt. % [27, 28].

**Synthesis of Rb[Co(hfac)$_3$] (1).** Samples of 0.181 g (0.619 mmol) of Rb(hfac) and 0.315 g (0.619 mmol) of [Co(H$_2$O)$_2$(hfac)$_2$] were dissolved together in 20 ml of diethyl ether. The resulting suspension was stirred for 4 h at room temperature. The target product was formed after evaporation of the red mother liquor. 0.420 g (0.549 mmol) of the complex was obtained. The yield was 90%. The results of elemental analysis (wt. %) are given below.

For $C_{15}H_3F_{18}O_6CoRb$ found, %: C 23.0; H 0.5; F 45.3;

Calculated, %: C 23.53; H 0.39; F 44.67.

IR spectrum (cm$^{-1}$): 1641, 1609, 1562, 1535, 1485 (ν(C=O) + ν(C=C)); 1256, 1201, 1142 (ν(CF)).

**Synthesis of [Rb(18C6)][Co(hfac)$_3$] (2).** Samples of 0.260 g (0.340 mmol) of Rb[Co(hfac)$_3$] and 0.090 g (0.340 mmol) of 18-crown-6 ether were dissolved together in 20 ml of dichloromethane. The resulting suspension was stirred for 4 h at room temperature, and the formation of a transparent red solution was observed. The target product crystallized upon evaporation of the solvent. 0.291 g (0.281 mmol) of the complex was obtained, with a yield of 80%. The results of elemental analysis (wt. %) are presented below.

For $C_{27}H_{27}F_{18}O_{12}RbCo$ found, %: C 31.7; H 3.1; F 32.6.

Calculated: C 31.49; H 2.64; F 33.21.

IR spectrum (cm$^{-1}$): 3035, 3020 (ν(C–H)); 1626, 1607, 1591, 1579, 1519, 1497 (ν(C=O) + ν(C=C)); 1222, 1207, 1145 (ν(CF)); 1095 (ν(C–O)).

**X-ray diffraction analysis** of synthesis products was carried out on a Bruker D8 Advance instrument (Cu $K_\alpha$-radiation, LynxEye XE-T detector, Bragg–Brentano

geometry, vertical θ–θ-goniometer, 2θ angle range 5 ° -70 ° , step 0.03 ° ) at room temperature. Polycrystals were ground dry in an agate mortar and packed into the recess of a standard cuvette. The diffractograms are shown in Fig. 1.

**X-ray structural analysis** of single crystals was performed on a Bruker D8 Venture single crystal diffractometer (three-circle goniometer, Incoatec IμS 3.0 microfocus source, Mo $K_\alpha$-radiation, focusing and monochromatization with Montel multilayer mirrors, Photon III CPAD detector, resolution 768 × 1024). The sample temperature was maintained using an Oxford Cryosystems Cryostream 800 plus nitrogen flow cryostat. Reflection intensities were measured by ω-scanning of narrow (0.5 ° ) frames. Absorption was accounted for semi-empirically using the SADABS software package [29]. The structures were solved by direct method and refined by full-matrix least squares method in anisotropic approximation for all non-hydrogen atoms using the SHELXL software complex [30]. Positions and thermal parameters of H atoms of organic anions and molecules were refined in the rigid body model. In the structure of [Rb(18C6)][Co(hfac)$_3$], positional disorder of one of the trifluoromethyl groups is present with site occupancies of 0.756(5) and 0.244(5). Atomic coordinates and other structural characteristics of Rb[Co(hfac)$_3$] and [Rb(18C6)][Co(hfac)$_3$] can be obtained from the Cambridge Structural Database ( deposit@ccdc.cam.ac.uk ), as well as in the supplementary materials (Tables 1S, 2S). The corresponding numbers, crystallographic characteristics, and details of diffraction experiments are given in Table 1. Some bond lengths and angle values are given in Table 2. Distortion of cobalt coordination polyhedra was evaluated using the SHAPE 2.1 program [31].

**Thermal analysis** of samples was performed on a Netzsch TG 209 F1 Iris thermal analyzer, supplied with the Proteus analysis software package. The sample weight was 10 ± 1 mg. Experiments were conducted in a helium atmosphere (30.0 ml/min, open $Al_2O_3$ crucible, 10 deg/min).

## RESULTS AND DISCUSSION

There are several approaches to obtaining heterometallic complexes containing alkali and transition metals.

Complexes without neutral ligands of the $M^{I}[M^{II}(hfac)_3$ type are well soluble in polar organic solvents (acetone, ethyl acetate). They are obtained by two methods: via the reaction of β -diketonate $M^{I}$ with an inorganic salt of $M^{II}$ or with the corresponding pre-synthesized β -diketonate. The first method is demonstrated in the synthesis of $K[Mn(hfac)_3$ from stoichiometric amounts of $Mn(NO_3)_2$ and K(hfac) in 96% ethanol with a yield of 70% after purification by vacuum sublimation [17]. The second method appears to be more universal: it has been successfully used to obtain not only $M^{I}[Co(hfac)_3$, $M^{I}$= K, Rb, Cs [18], but also a wide range of complexes $Cs[M^{II}(\beta\text{-dik})_3$, where $M^{II}$ = Mn, Co, Ni, Zn; β -dik = hfac, tfac (1,1,1-trifluoropentanedionate-2,4) and acac (pentanedionate-2,4) [19]. The synthesis was carried out in methanol, where the target products formed as precipitates ( β -dik = tfac, acac) or were salted out with chloroform ( β -dik = hfac), and possible impurities of the initial *bis* -chelates were distilled off in vacuum. However, the yield, and for $M^{I}$= K, Rb, the data of primary characterization of products were not provided. It should be noted that crystals of $K[M^{II}(hfac)_3$ ($M^{II}$= Co [21] and Ni [32]) were obtained as by-products in the synthesis of polynuclear mixed-ligand complexes.

Thus, for the synthesis of $Rb[Co(hfac)_3$ ( **1** ) in this work, the second approach was implemented with the replacement of the solvent with diethyl ether, resulting in a yield of ~90%.

Since cations in heterometallic complexes with neutral ligand of type $[M^{I}(Q)][M(hfac)_n]$ are surrounded by large organic molecules Q, this leads to their better solubility in non-coordinating organic solvents (chloroform, dichloromethane). This feature is used in the only known approach to synthesizing such complexes:

[Na(tetraglyme)][$M^{III}$(hfac)$_4$] ($M^{III}$ = Y, Gd) were obtained through *in situ* self-assembly when boiling in dichloromethane [22]. The sequence of adding reagents likely affects the composition of products: first, a neutral ligand was added to the suspension of $M^{III}(NO_3)_3 \cdot 6H_2O$, and only after holding - NaOH (10% excess) and Hhfac. The yield of target products was ~80%.

In our case, an attempt to synthesize [Rb(18C6)][Co(hfac)$_3$] ( **2** ) by reacting Rb(hfac), [Co($H_2O$)$_2$(hfac)$_2$] and 18C6 in dichloromethane (simultaneous dissolution) led to obtaining a red oily liquid that did not crystallize for >2 months (including at –20°C), which made it impossible to determine the composition and single-phase nature of the product. In contrast, the approach based on breaking the polymer chain with a polydentate ligand, i.e., on direct heterophase reaction of Rb[Co(hfac)$_3$] with 18C6, proved effective - the yield of **2** was ~80%.

Complexes **1** and **2** are red and orange powders respectively, stable when stored in air. Both complexes do not contain water in their composition, which is confirmed by IR spectroscopy (absence of both symmetric and asymmetric O-H stretching vibrations in the 3400-3200 $cm^{-1}$ region). IR spectra also show characteristic vibrations of β-diketonate fragments: ν(C=O) + ν(C=C) in the 1650-1500 $cm^{-1}$ region and ν(C-F) in the 1300-1100 $cm^{-1}$ region. A notable difference in the spectra is the presence of absorption bands in complex **2** corresponding to crown ether group vibrations at 3065, 3020 $cm^{-1}$ (ν(C-H)) and 1095 $cm^{-1}$ (ν(C-O), intense). The assignment of Co-O bond stretching vibration bands is ambiguous: a medium intensity band at 723 $cm^{-1}$ is present in the spectrum of **2** and corresponds to literature data for [Co(hfac)$_3$]$^-$ complexes with organic counterion, such as $NEt_4^+$ [33], as well as calculations for mixed-ligand octahedral Co(II) complexes [34]. However, in the spectrum of **1** such band is absent, and a band of comparable intensity at 671 $cm^{-1}$ and a low-intensity band at 745 $cm^{-1}$ are observed. Since Co-O bond lengths in both

complexes are similar (see below), such changes can be attributed to differences in coordination polyhedra distortion or crystal packing.

Elemental and X-ray phase analysis data (Fig. 1) unambiguously confirm the composition and single-phase nature of the complexes. Note that the Rietveld refinement [35] showed that the considered phase **1** corresponds to experimental data (Supplementary materials, Fig. 1S). Crystals suitable for XRD were obtained after evaporation of the solvent during synthesis.

**Rb[Co(hfac)$_3$]** crystallizes in monoclinic system, sp. gr. $P2_1/n$ (Fig. 2a). The independent part includes one $Rb^+$, $Co^{2+}$ cation and three hfac-anions. All β-diketonate ligands are coordinated to the cobalt cation in a bidentate-cyclic manner, forming complex anions $[Co(hfac)_3]^-$ with a distorted octahedral polyhedron $\{CoO_6\}$. The Co–O bond lengths lie within a narrow range of 2.043(5)–2.058(5) Å. The rubidium cation environment consists of three O atoms and two F atoms of one $[Co(hfac)_3]^-$ anion, as well as three O atoms of the adjacent $[Co(hfac)_3]^-$ anion. The $\{RbO_6F_2\}$ polyhedron represents a triangular antiprism (with O(11), O(21), O(31) atoms at the base) with two caps (F(21) and F(31)). The Rb–O and Rb–F distances are in the ranges of 2.931(5)–3.028(5) and 3.153(7)–3.190(6) Å, respectively. Additionally, there are four elongated Rb…F contacts: 3.226(7) Å with the $[Co(hfac)_3]^-$ anion providing F atoms to the rubidium coordination polyhedron, and 3.277(6), 3.293(8), 3.451(6) Å with the adjacent anion. Thus, chains of rubidium cations and complex anions are formed (Fig. 2b), connected through Rb…F (2 + 4 pcs.) and Rb…O (6 pcs.) contacts along the ( 11 0) direction. They are arranged in a hexagonal pattern (Fig. 3).

Comparison with the analog $K[Co(hfac)_3]$ [21] shows that, although the structures were studied at different temperatures (Table 2), the $Co–O_{hfac}$ distances coincide within the margin of error, the OCoO chelate angles and geometric characteristics of hfac-ligands are similar. The CShM indices, showing deviation

from the ideal polyhedron, in our case octahedron {$CoO_6$}, differ slightly. Thus, the increase in $M^I$ radius = K < Rb in the structures $M^I[Co(hfac)_3]$ leads to the formation of a more regular figure. The $M^I$–$O_{hfac}$ and $M^I$–F distances naturally increase with the growth of the cation ionic radius. The number of corresponding $M^I$…O contacts in the chains remains constant, while for $M^I$ = K, a greater variety of $M^I$…F contacts is characteristic: 2 + 4, 3 + 3, 3 + 0 pieces compared to 2 + 4 pieces for $M^I$ = Rb. Overall, the increase in the alkali metal cation $M^I$ radius leads to a decrease in crystal symmetry ( $P\,3\,c \rightarrow P\,2_1/n$ ).

**[Rb(18C6)][Co(hfac)$_3$]** crystallizes in the monoclinic system, space group $P\,2_1/n$ (Fig. 4a). The independent part includes one 18C6 ligand, one $Rb^+$ and $Co^{2+}$ cation each, three hfac-anions.

All β-diketonate ligands are coordinated to the cobalt cation in a bidentate-cyclic manner, forming complex anions $[Co(hfac)_3]]^-$ with a distorted octahedral polyhedron {$CoO_6$}. The Co–O bond lengths lie in the range of 2.0517(17)–2.0854(18) Å (average 2.07 Å).

The Rb(1) environment consists of six O atoms from the crown ether and two F atoms from two different $[Co(hfac)_3]^-$ anions. The {$RbO_6F_2$ polyhedron represents a hexagonal bipyramid (one vertex is F(11) atom, the second vertex is one of the disordered fluorine atoms (F(14A) or F(16B)), the base of the bipyramid consists of O(401)–O(406) atoms. The Rb–$O_{(18C6)}$ distances are in the range of 2.8506(17)–2.9205(19) Å (average 2.89 Å). The $Rb^+$ cation is displaced from the mean cavity of the crown ether (constructed using all atoms) by 0.745 Å. The average C–$O_{(18C6)}$ and C–$C_{(18C6)}$ bond lengths are 1.42(4) and 1.49(5) Å respectively, with the latter being shortened compared to typical C–C bonds in aliphatic compounds (1.54 Å). This is consistent with the data on crown ether complexation [35, 36].

[Rb(18C6)]$^{+}$ cations and [Co(hfac)$_3$]$^{-}$ anions are connected by Rb…F contacts with lengths of 2.9129(17)–2.992(14) Å, forming chains along the *a* axis. These chains are arranged in a hexagonal pattern (Fig. 5) similar to **1** .

Overall, the geometric parameters of the nearest cobalt environment and hfac-ligands in complexes **1** and **2** are close, for example, the bond lengths match within 0.02 Å (Table 2). At the same time, the CShM index shows that in complex **2** the {CoO$_6$ polyhedron is more regular. As a result of crown ether inclusion, the Co…Rb distances significantly increase (3.697–3.719 Å ( **1** ) << 6.389 Å ( **2** )), Rb–O contacts between the cation and complex anion disappear, and the total number of Rb…F contacts decreases to two. Meanwhile, the shortest Rb–F distances decrease by ~0.15 Å. Thus, the introduction of the neutral ligand 18C6 leads to a significant decrease in calculated density (2.057 ( **1** ) → 1.784 g/cm$^3$ ( **2** )), i.e., to structure "loosening".

The thermal properties of heterometallic complexes **1** and **2** compared to the initial Rb(hfac) and [Co(H$_2$O)$_2$(hfac)$_2$] were studied by thermogravimetry in the temperature range of 25-750°C. The experiments were conducted in an inert atmosphere (helium) with a constant heating rate (10 degrees/min). The mass loss curves are shown in Fig. 6, brief results of thermal properties analysis are presented in Table 3.

The Rb(hfac) complex apparently absorbs water, as indicated by gradual mass loss in the temperature range of 50-130°C (the calculation agrees with the stoichiometry Rb(hfac) · 0.5H$_2$O). The dehydrated complex is stable in the temperature range up to 180°C, after which it decomposes in one step. Although the final mass residue value does not correspond to calculations for RbF (Table 2), previous studies [23, 25, 38] show that this is the most probable decomposition product. The smooth course of the mass loss curve at temperatures >350°C may correspond to thermal annealing of carbon-containing decomposition products. In contrast, the [Co(H$_2$O)$_2$(hfac)$_2$] complex transitions to the gas phase quantitatively

in the range of 80-240°C, therefore the decomposition temperature could not be recorded. Note that the mass loss curve does not contain an explicit step of coordinated $H_2O$ molecules detachment.

Mass constancy of **1** and **2** at temperatures up to 200°C confirms the absence of water in the composition, which is consistent with elemental analysis and IR spectroscopy data. Both heterometallic complexes are thermally more stable than Rb(hfac) and less volatile than $[Co(H_2O)_2(hfac)_2]$. The latter, as well as the general shape of the mass loss curve for $Rb[Co(hfac)_3]]$ ( **1** ) are consistent with data from [19]. The crown ether complex ( **2** ) decomposes in one stage in the temperature range of 200-400°C, apparently to $RbCoF_3$ (Table 2), while **1** predominantly transitions to the gas phase at 240-400°C (mass residue 6.1% << calculated value 26.3% for $RbCoF_3$). The increased thermal stability of the $Rb[Co(hfac)_3]$ complex in the condensed phase is probably due to the large number of intrachain contacts. Most likely, complex **1** exists in the gas phase as an isolated fragment of $Rb[Co(hfac)_3]$. For example, related chain complexes $K[Ln(hfac)_4]$ (Ln = La, Gd, Lu) have been shown to split into corresponding ion pairs where the cation and anion are connected by three K…O and K…F contacts [39]. In complex **2** , the presence of crown ether in the rubidium coordination sphere may hinder such contacts, i.e., reduce the stability of the ion pair.

Note that the vacuum sublimation test for the complexes under identical conditions ( $t$ = 180 °C, $P = 10^{-2}$ Torr) showed that **1** transitions to the gas phase quantitatively, while for **2** , 47% of the initial sample condenses. According to XRD and IR spectroscopy data, the sublimation product in both cases is $Rb[Co(hfac)_3]$ (Fig. S2, S3). Thus, there is a detachment of the neutral ligand in **2** (according to calculated data, 18C6 losses are 25.6%) and partial sublimation of **1** . Determining the sequence of these transformations requires investigation of the gas phase of the complexes.

## CONCLUSION

Complexes $Rb[Co(hfac)_3]$ and for the first time $[Rb(18C6)][Co(hfac)_3]$ were synthesized, their crystal structures and thermal properties were studied. Both complexes have a chain polymer structure.

It was shown that for $M^I[Co(hfac)_3]$, where $M^I$ = K and Rb, the structure of the complex anion remains unchanged, the structural organization of the chains is generally similar due to cation contacts with O atoms (6 pcs.) and F (2-6 pcs.). The distances $M^I$-$O_{hfac}$ and $M^I$-F naturally increase with increasing ionic radius, while the number of contacts does not correspond to this trend. The addition of the polydentate ligand 18C6 leads to the filling of the coordination environment of $Rb^+$, therefore the cationic and anionic fragments in the complex $[Rb(18C6)][Co(hfac)_3]$ are connected only through Rb-F contacts (2 pcs.). Changes in the structure affect solubility. Thus, the complex with 18C6, unlike $M^I[Co(hfac)_3]$, dissolves in non-coordinating solvents (chloroform, dichloromethane).

TGA showed that the thermal stability of the complexes increases in the series $Rb(hfac) < [Rb(18C6)][Co(hfac)_3] < Rb[Co(hfac)_3]$. The complex $Rb[Co(hfac)_3]$, unlike the others, transitions to the gas phase with partial decomposition already at atmospheric pressure, making it promising for testing in MOCVD deposition processes of corresponding fluoroperovskites. The complex $[Rb(18C6)][Co(hfac)_3]$ can be used for solid-phase synthesis of $RbCoF_3$.

## ACKNOWLEDGMENT

The authors are grateful to the Chemical Research Shared Facility Center SB RAS (NIOCH SB RAS) for performing elemental analysis.

## FUNDING

This work was supported by the Ministry of Science and Higher Education of the Russian Federation under projects No. 121031700314-5 and 121031700313-8.

## CONFLICT OF INTEREST

The authors declare that they have no conflict of interest.

## ADDITIONAL INFORMATION

The online version contains supplementary materials available at https://doi.org/

## REFERENCES

1. *Steblevskaya N.I., Ziatdinov A.M., Belobeletskaya M.V. et al.* // Russ. J. Inorg. Chem. 2023. V. 68. P. 1737. https://doi.org/10.1134/S0036023623602210

2. *Lin K., Xing J., Quan L.N. et al.* // Nature. 2018. V. 562. P. 245. https://doi.org/10.1038/s41586-018-0575-3

3. *Wehrenfennig C., Eperon G.E., Johnston M.B. et al.* // Adv. Mater. 2014. V. 26. No. 10. P. 1584. https://doi.org/10.1002/adma.201305172

4. *Zeng J., Li X., Wu Y. et al.* // Adv. Funct. Mater. 2018. V. 28. P. 1804394. https://doi.org/10.1002/adfm.201804394

5. *Xu Y., Cao M., Huang S.* // Nano Res. 2021. V. 14. P. 3773. https://doi.org/10.1007/s12274-021-3362-7

6. *Temerov F., Baghdadi Y., Rattner E. et al.* // ACS Appl. Energy Mater. 2022. V. 5. No. 12. P. 14605. https://doi.org/10.1021/acsaem.2c02680

7. *Wang H., Zhang X., Wu Q. et al.* // Nat. Commun. 2019. V. 10. No. 1. P. 665. https://doi.org/10.1038/s41467-019-08425-5

8. *Körbel S., Marques M.A.L., Botti S.* // J. Mater. Chem. C. 2016. V. 4. No. 15. P. 3157. https://doi.org/10.1039/C5TC04172D

9. *Mubarak A.A.* // Mod. Phys. Lett. B. 2017. V. 31. No. 6. P. 1750033. https://doi.org/10.1142/s0217984917500336

10. *Erum N., Iqbal M.A* . // Acta Phys. Pol. A. 2020. V. 138. No. 3. P. 509. https://doi.org/10.12693/APhysPolA.138.509

11. *Hashmi R., Zafar M., Shakil M. et al.* // Chin. Phys. B. 2016. V. 25. No. 11. P. 117401. https://doi.org/10.1088/1674-1056/25/11/117401

12. *Shafer M.W.* // J. Appl. Phys. 1969. V. 40. No. 3. P. 1601. https://doi.org/10.1063/1.1657792

13. *Dubrovin R.M., Siverin N.V., Syrnikov P.P. et al.* // Phys. Rev. B. 2019. V. 100. No. 2. P. 024429. https://doi.org/10.1103/physrevb.100.024429

14. *Parhi P., Kramer J., Manivannan V.* // J. Mater. Sci. 2008. V. 43. No. 16. P. 5540. https://doi.org/10.1007/s10853-008-2833-5

15. *Munasinghe H.N., Suescun L., Dhanapala B.D. et al.* // Inorg. Chem. 2020. V. 59. No. 23. P. 17268. https://doi.org/10.1021/acs.inorgchem.0c02522

16. *Dhanapala B.D., Munasinghe H.N., Suescun L. et al.* // Inorg. Chem. 2017. V. 56. No. 21. P. 13311. https://doi.org/10.1021/acs.inorgchem.7b02075

17. *Troyanov S.I., Gorbenko O.Y., Bosak A.A* . // Polyhedron. 1999. V. 18. No. 26. P. 3505. https://doi.org/10.1016/S0277-5387(99)00288-0

18. *Gurevich M.Z., Sas T.M., Mazepova N.E. et al.* // Zhurn. neorgan. khimii. 1975. V. 20. No. 3. P. 735.

19. *Gurevich M.Z., Sas T.M., Stepin B.D. et al.* // Zhurn. neorgan. khimii. 1971. V. 16. No. 6. P. 1748.

20. *Makarenko A.M., Zaitsau D.H., Zherikova K.V.* // Coatings. 2023. V. 13. No. 3. P. 535. https://doi.org/10.3390/coatings13030535

21. *Kuznetsova O.V., Fursova E.Y., Letyagin G.A et al.* // Russ. Chem. Bull. 2018. V. 67. No. 7. P. 1202. https://doi.org/10.1007/s11172-018-2202-8

22. *Battiato S., Rossi P., Paoli P. et al.* // Inorg. Chem. 2018. V. 57. No. 24. P. 15035. https://doi.org/10.1021/acs.inorgchem.8b02267

23. *Peddagopu N., Sanzaro S., Rossi P. et al.* // Eur. J. Inorg. Chem. 2021. V. 2021. No. 36. P. 3776. https://doi.org/10.1002/ejic.202100553

24. *Gulino A., Fiorito G., Fragalà I.* // J. Mater. Chem. 2003. V. 13. No. 4. P. 861. https://doi.org/10.1039/b211861k

25. *Kochelakov D.V., Vikulova E.S., Kuratieva N.V. et al.* // J. Struct. Chem. 2023. V. 64. P. 82. https://doi.org/10.1134/S0022476623010055

26. *Nakamoto K.* Infrared and Raman spectra of inorganic and organic compounds. USA, New York: John Wiley & Sons Inc., 1997.

27. *Mikhailovskaya T.F., Makarov A.G., Selikhova N.Y. et al.* // J. Fluorine Chem. 2016. V. 183. P. 44. https://doi.org/10.1016/j.jfluchem.2016.01.009

28. *Tikhova V.D., Fadeeva V.P., Nikulicheva O.N. et al.* // Chem. Sust. Develop. 2022. V. 30. P. 640. https://doi.org/10.15372/CSD2022427

29. APEX3 (v.2019.1-0), Bruker AXS Inc., Madison, Wisconsin, USA, 2019.

30. *Sheldrick G.M.* // Acta Crystallogr., Sect. C: Struct. Chem. 2015. V. 71. No. 1. P. 3. https://doi:10.1107/S2053229614024218

31. *Casanova D., Llunell M., Alemany P. et al.* // Chem.-Eur. J. 2005. V. 11. No. 5. P. 1479. https://doi.org/10.1002/chem.200400799

32. *Fursova E.Y., Kuznetsova O.V., Ovcharenko V.I. et al.* // Russ. Chem. Bull. 2008. V. 57. No. 6. P. 1198. https://doi.org/10.1007/s11172-008-0151-3

33. *Palii A.V., Korchagin D.V., Yureva E.A. et al.* // Inorg. Chem. 2016. V. 55. No. 19. P. 9493. https://doi.org/10.1021/acs.inorgchem.6b01473

34. *Klotzsche M., Barreca D., Bigiani L. et al.* // Dalton Trans. 2021. V. 50. P. 10374. https://doi.org/10.1039/D1DT01650D

35. *Rietveld H.M.* // J. Appl. Crystallogr. 1969. V. 2. P. 65. https://doi.org/10.1107/S0021889869006558

36. *Pedersen C.J.* // J. Am. Chem. Soc. 1967. V. 89. No. 26. P. 7017. https://doi.org/10.1021/ja01002a035

37. *Norov Sh.K.* Complex-forming and membrane-active properties of crown ethers. Tashkent: Fan, 1991. 60 p. ISBN 5-648-01316-7

38. *Peddagopu N., Pellegrino A.L., Bonaccorso C. et al.* // Molecules. 2022. V. 27. No. 19. P. 6282. https://doi.org/10.3390/molecules27196282

39. *Girichev G.V., Giricheva N.I., Khochenkov A.E. et al.* // Chem. Eur. J. 2021. V. 27. No. 3. P. 1103. https://doi.org/10.1002/chem.202004010

**Table 1.** Crystallographic data and experimental conditions for $RbCo(hfac)_3$ and $[Rb(18C6)][Co(hfac)_3]$

| Parameter | $RbCo(hfac)_3$ | $[Rb(18C6)][Co(hfac)_3]$ |
|---|---|---|
| Stoichiometric formula | $C_{15}H_3F_{18}O_6RbCo$ | $C_{27}H_{27}F_{18}O_{12}RbCo$ |
| $M$, g/mol | 765.57 | 1029.88 |
| Crystal size, mm | 0.10 × 0.08 × 0.04 | 0.13 × 0.07 × 0.03 |
| $T$, K | 150(2) | 150(2) |
| Crystal system | Monoclinic | Monoclinic |
| Space gr. | $P2_1/n$ | $P2_1/n$ |
| $a$, Å | 12.2962(14) | 12.4720(2) |
| $b$, Å | 16.858(2) | 20.6154(3) |
| $c$, Å | 12.4313(13) | 15.7584(2) |
| α, deg | 90 | 90 |
| β, deg | 106.390(5) | 108.8130(10) |
| γ, deg | 90 | 90 |
| $V$, Å$^3$ | 2472.2(5) | 3835.27(10) |
| $Z$ | 4 | 4 |
| Density (calculated), g/cm$^3$ | 2.057 | 1.784 |
| Absorption coefficient, mm$^{-1}$ | 2.816 | 1.852 |
| Data collection range 2 θ, deg | From 2.092 to 25.685 | From 1.685 to 27.491 |
| Range $h, k, l$ | $-14 \le h \le 14$<br>$-20 \le k \le 19$<br>$-13 \le l \le 15$ | $-15 \le h \le 16$<br>$-26 \le k \le 17$<br>$-20 \le l \le 19$ |
| Number of measured reflections | 10925 | 29604 |
| Number of independent reflections | 4640 | 8716 |
| $R_{int}$ | 0.0542 | 0.0333 |
| Data collection completeness ( θ = 25.25°), % | 98.9 | 99.2 |
| Max. and min. transmission | 0.526 and 0.745 | 670 and 0.746 |
| No. of reflns/restr./params. | 4640/0/347 | 8716/1/555 |
| $S$-factor on $F^2$ | 1.066 | 1.068 |
| $R$-factor [ $I > 2\sigma(I)$] | $R_1 = 0.0734$<br>$wR_2 = 0.1966$ | $R_1 = 0.0381$<br>$wR_2 = 0.0886$ |
| $R$-factor (all data) | $R_1 = 0.1403$<br>$wR_2 = 0.2202$ | $R_1 = 0.0563$<br>$wR_2 = 0.0933$ |
| Max. and min. residual density, $e$ /Å$^3$ | 0.915 and –0.684 | –0.552 and 1.345 |

| CCDC number | 2374818 | 2374819 |
|---|---|---|

**Table 2.** Some bond lengths and angles in complexes $M^{I}[Co(hfac)_3]$, where $M^{I}$ = K, Rb, and [Rb(18C6)][Co(hfac)$_3$]

| Parameter | K[Co(hfac)$_3$] [21] | Rb[Co(hfac)$_3$] | [Rb ( 18C6 ) [Co(hfac)$_3$] |
|---|---|---|---|
| $T$, K | 295 | 150 | 150 |
| Co–O$_{hfac}$, Å | 2.035(10)–2.070(10) <2.05> | 2.043(5)–2.058(5) <2.05> | 2.052(2)–2.085(2) <2.07> |
| $M^{I}$–O$_{hfac}$, Å | 2.773(16)–2.802(12) <2.79> | 2.931(5)–3.028(5) <2.97> | — |
| $M^{I}$–F, Å | 3.095(16) | 3.190(6)–3.153(7) | 2.913(3)–2.992(1) |
| Rb–O$_{(18C6)}$ | — | — | 2.851(2)–2.921(2) <2.89> |
| C–O$_{hfac}$, Å | 1.23(2)–1.261(18) <1.245> | 1.255(8)–1.284(8) <1.264> | 1.237(3)–1.254(3) <1.246> |
| C–C$_{\gamma}$, Å | 1.34(3)–1.43(3) <1.378> | 1.373(10)–1.393(10) <1.379> | 1.378(4)–1.399(4) <1.389> |
| C–C, Å | 1.520(18)–1.56(2) <1.535> | 1.470(12)–1.558(10) <1.516> | 1.530(4)–1.538(3) <1.534> |
| C–C$_{(18C6)}$ | — | — | 1.486(4)–1.500(4) <1.49> |
| C–O$_{(18C6)}$ | — | — | 1.417(3)–1.438(3) <1.42> |
| ∠OCoO$_{chel}$, deg | 87.5(5)–88.2(5) <87.9> | 88.3(2)–88.6(2) <88.4> | 88.1(6)–88.8(7) <88.5> |
| CShM Index | 0.499 | 0.396 | 0.078 |

**Table 3.** Brief results of thermogravimetric data analysis for Rb(hfac), [Co(H$_2$O)$_2$(hfac)$_2$], Rb[Co(hfac)$_3$] and [Rb(18C6)][Co(hfac)$_3$]

| Complex | $t_{water\ loss}$, °C | $H_2O$ loss exp.(calc.), % | $t_{mass\ loss\ onset}$, °C | Mass residue exp.(calc.), % |
|---|---|---|---|---|
| Rb(hfac) | 50-130 | 3.0 (3.0-0.5 $H_2O$) | 180 | 44.3 (34.6, RbF) |
| [Co(H$_2$O)$_2$(hfac)$_2$] | - | - | 80 | 0.0 (19.4, $CoF_2$) |
| Rb[Co(hfac)$_3$] ( **1)** | - | - | 240 | 6.1 (26.3, $RbCoF_3$) |
| [Rb(18C6)][Co(hfac)$_3$](**2)** | - | - | 200 | 20.8 (19.6 $RbCoF_3$) |

FIGURE CAPTIONS

**Fig. 1.** Diffraction patterns of synthesis products **1** and **2** .

**Fig. 2.** Fragment of Rb[Co(hfac)$_3$] chain (a), chains in direction ( 11 0) (b).

**Fig. 3.** Hexagonal packing motif of Rb[Co(hfac)$_3$chains.

**Fig. 4.** Fragment of [Rb(18C6)][Co(hfac)$_3$chain (a), chains along *a* direction shown without positional disorder for clarity (b).

**Fig. 5.** Hexagonal motif of [Rb(18C6)][Co(hfac)$_3$] (perpendicular to *a* axis).

**Fig. 6.** Thermograms of Rb(hfac), [Co(H$_2$O)$_2$(hfac)$_2$], Rb[Co(hfac)$_3$] and [Rb(18C6)][Co(hfac)$_3$] (He atmosphere, heating rate 10 degrees /min).

(б)

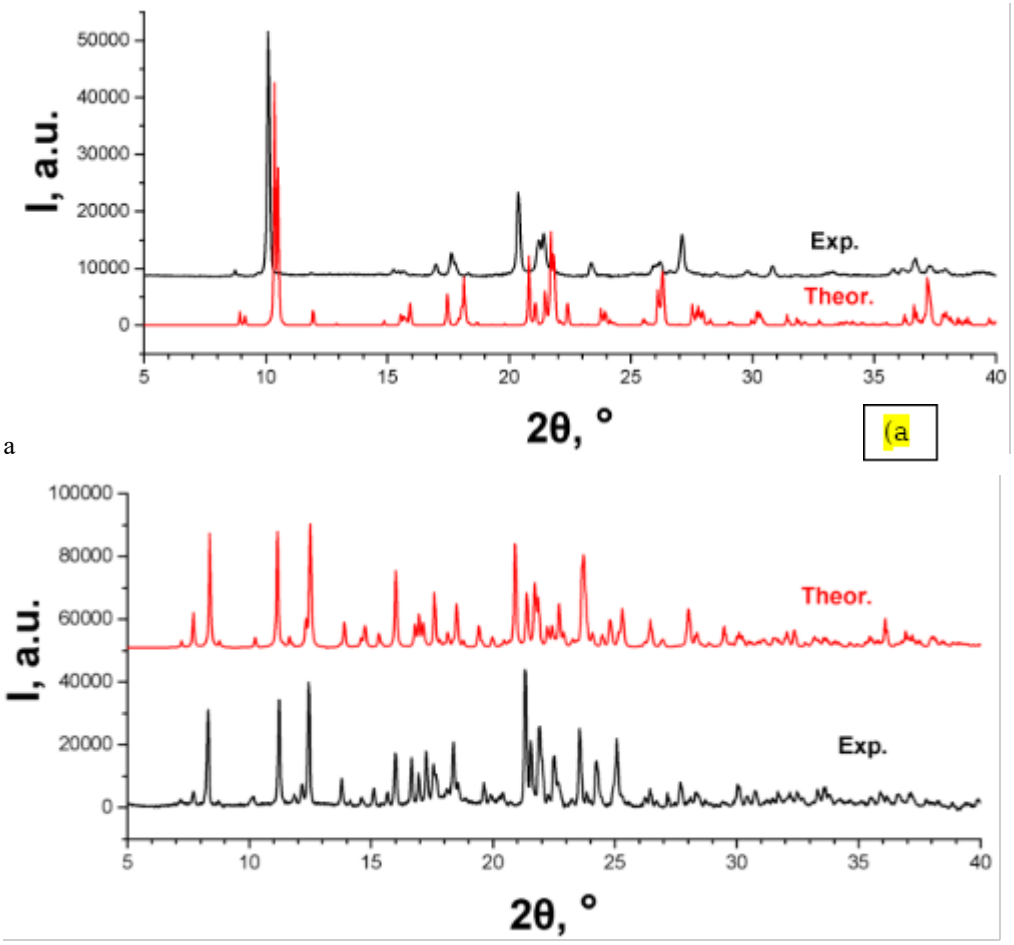


a

(а

b

Fig. 1. Kochelakov

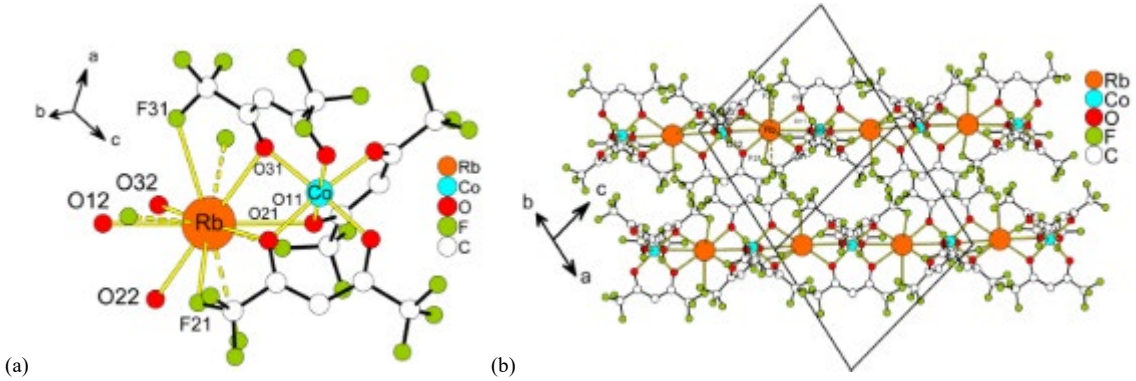


(a) (b)

Fig. 2. Kochelakov

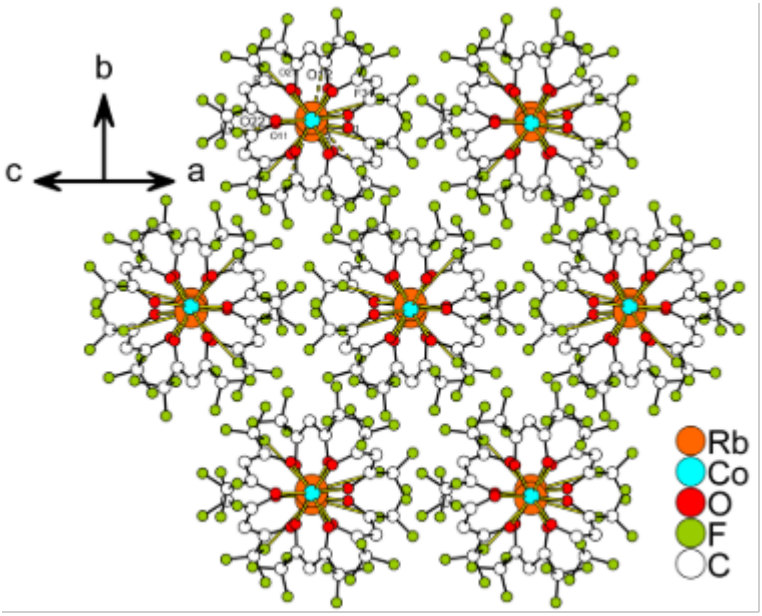


Fig. 3. Kochelakov

(a)

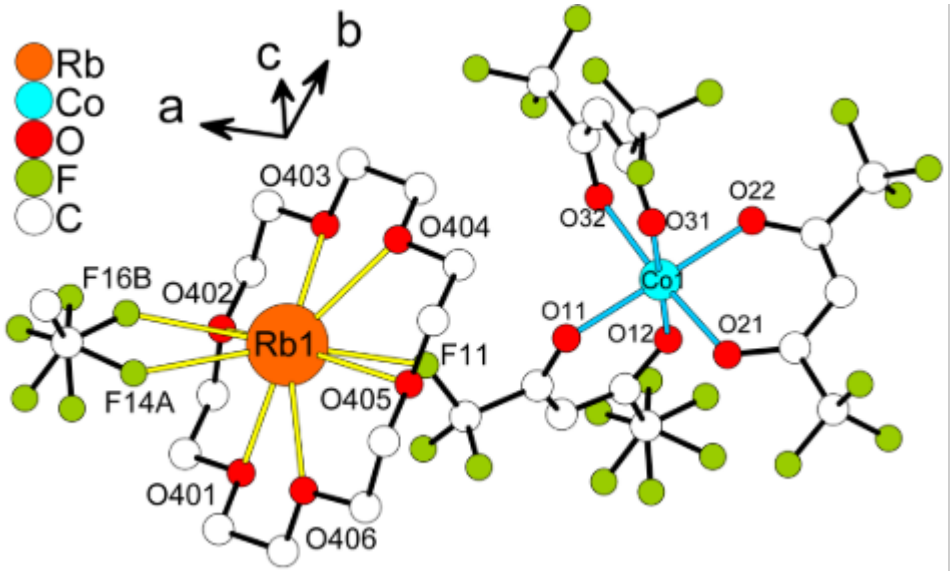


(b)

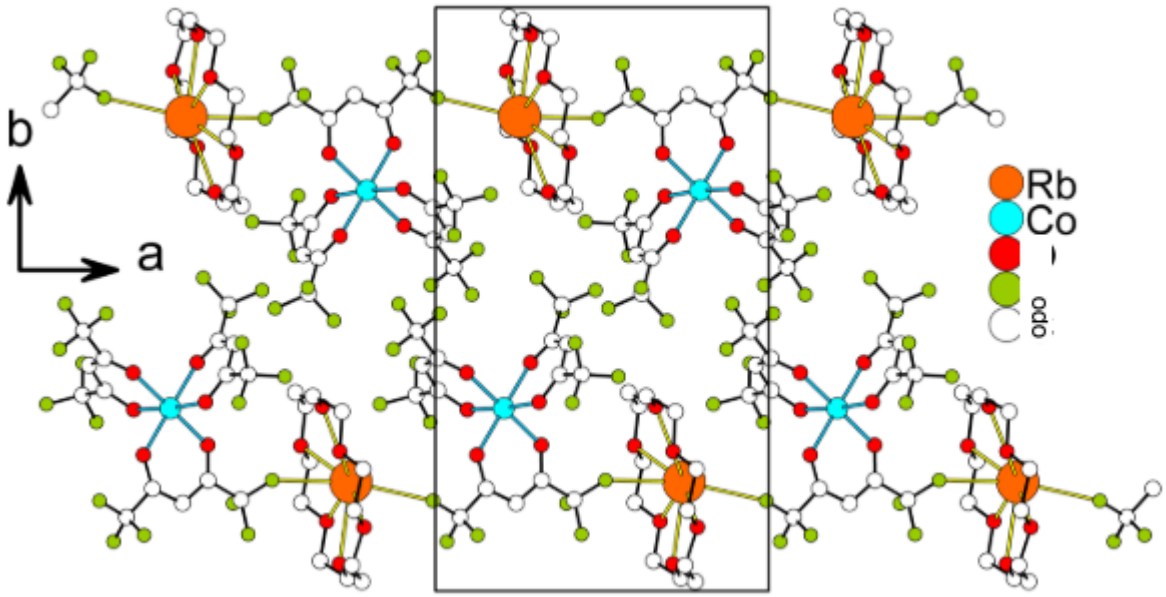


Fig. 4. Kochelakov

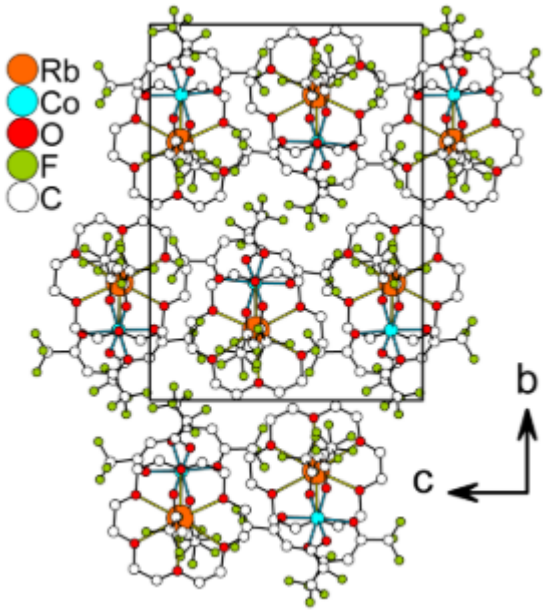


Fig. 5. Kochelakov

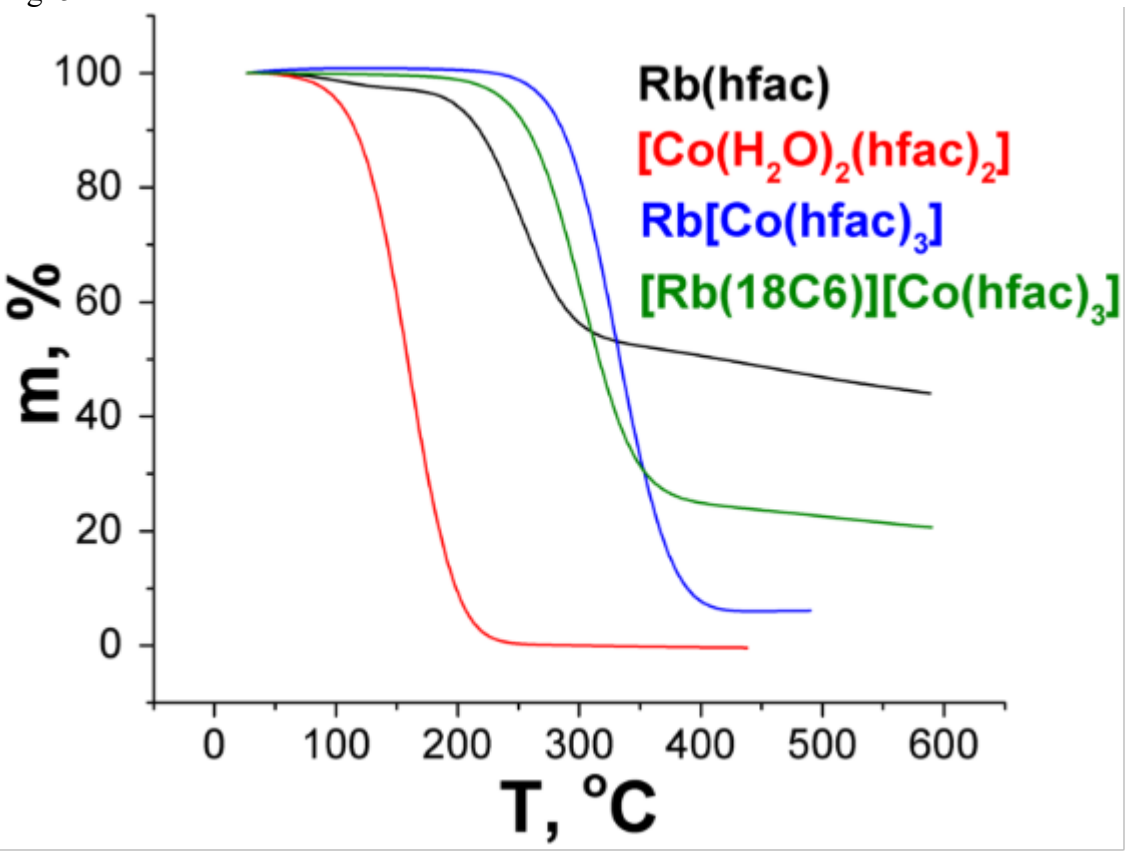


Fig. 6. Kochelakov